Asian Journal of Chemistry; Vol. 24, No. 11 (2012), 4907-4910

ASIAN JOURNAL OF CHEMISTRY

www.asianjournalofchemistry.co.in

Electrochemical Characterization of Nanostructured Polyaniline-PbO_2 Composite Prepared by Cyclic Voltammetry

PHAN THI BINH*, MAI THI THANH THUY, TRAN HAI YEN and PHAM THI TOT

Institute of Chemistry, Vietnamese Academy of Science and Technology, 18 Hoang Quoc Viet, Hanoi, Vietnam

*Corresponding author: Fax: +84 43 8361283; Tel: +84 43 7564312; E-mail: ptbinh@ich.vast.ac.vn

(*Received*: 19 July 2011; *Accepted*: 30 May 2012) AJC-11525

PANi-PbO_2 composites were prepared onto stainless steel substrate by cyclic voltammetry from acidic medium (potential range: 1.2-1.7 V; scan rates: 50-150 mV/s). The electrochemical properties of those materials were evaluated by cyclic potentiodynamic polarization (±150 mV to zero potential), cyclic voltammetry (potential range from 0.7 V to 1.8 V at scan rate of 100 mV/s) and impedance spectroscopy following potential from 1.5 V to 1.8 V (frequences: 100 kHz-10 mHz; amplitude: 5mV). There were found two electrical equivalent schemas by simulation that containing Warburg diffusion for potential area from 1.5 V to 1.6 V and without it for potential from 1.7 V to 1.8 V, respectively. The results showed that the formation of both α and β-modifications of lead dioxide in composite depended on scan rate at which samples synthesized and their electrochemical redoxidation peaks increased following cycle number of cyclic voltammetry due to the presence of polyaniline in composite matrix. The material that performanced at 100 mV/s had the best corrosion stability among regarded samples because of having the smallest corrosion current and the positive corrosion potential.

Key Words: PANi-PbO_2 composite, Cyclic voltammetry, Impedance spectroscopy, Cyclic potentiodynamic polarization.

INTRODUCTION

There is a considerable interest in fabricating organic-inorganic hybrid materials, which based on polyaniline (PANi) and inorganic metal oxides for many applications such as battery fabrication[1,2], electrocatalysis[3], sensor preparation[4] and new material development[5,6]. They can be gained by differrent ways such as spin coating method[7], chemical preparation[8] and electrochemical performance[9]. Among them PbO_2-PANi composite may be excellent candidate not only as cathode material for secondary batteries but also as anode for electrocatalytic oxidation of some organic compounds due to having high electrical conductivity, large oxygen overpotential and inexpensive price of lead dioxide. The better relevation of preparing those composites may be cyclic voltammetric method that has some advandtages over the others such as varying firstly potential range at which no oxygen gas develops, secondly potential scan rate which influences on forming morphology of material and thirdly cycle number which can make changing not only the thickness but also morphology of films. Comparatively less reports are available on the electrochemical properties of nanostructured composite synthesized by cyclic voltammetry.

This paper will report some results about electrochemical properties such as potentiodynamic polarization, cyclic voltammetry and impedance behaviour of PbO_2-PANi performanced by cyclic voltammetry at differrent scan rates.

EXPERIMENTAL

Analytical grade nitric acid, sulfuric acid, $Cu(NO_3)_2$, $Pb(NO_3)_2$, ethylene glycol (Merk) were used without any purification. Aniline (Merk) was freshly distilled under water vacuum condition at *ca.* 120 ºC before using. The cyclic voltammetric method was applied to electrosynthesis of PbO_2-PANi composite on an electrochemical work station system IM6 from Zahner Elektrik unit (Germany) in the voltage range from 1.2 V to 1.7 V *versus* Ag|AgCl|saturated KCl electrode.

PbO_2-PANi composites on stainless steel (SS) electrode were prepared by reported procedure[10]. After finishing, the films were washed by distilled water, immersed in acetone to remove the excess of aniline and then brought to characterize their electrochemical properties in 0.5 M sulfuric acid solution.

Electrochemical measurements were performed using an electrochemical workstation IM6 (Zahner-Elektrik). All experiments were carried out at room temperature in a three electrode system. A SS|PANi-PbO_2 was used as a working electrode. The counter electrode was the platine net. The Ag|AgCl|saturated KCl was employed as the reference electrode (0.1976 V *vs.* standard hydrogen electrode) and 0.5 M H_2SO_4 solution as electrolyte for measuring. The electrochemical properties of those composites were characterized by cyclic voltammetry at scan rate of 100 mV/s in the potential area of 0.7-1.8 V, cyclic potentiodynamic polarization (±150 mV to zero potential) and impedance spectroscopy following potential from 1.5 V to 1.8 V in anodic direction (frequencies: 100 kHz-10 mHz; amplitude: 5mV).

RESULTS AND DISCUSSION

Cyclic potentiodynamic polarization: Corrosion parameters such as corrosion potential (E_{corr}) and corrosion current density (i_{corr}) were extrapolated by Tafel-line[11] from curves on Fig. 1. Among them E_{corr} value is indicative for the ionization tendency of materials in specific media. The ionization tendency is decreased towards higher E_{corr} values. In standard potentiodynamic polarization tests, pitting tendency is evaluated by not only pitting potential but also the type of hysteresis in reverse scan[12,13]. A hysteresis loop is completed when the profile of the reverse potential scan intersects the positive potential scan where pitting corrosion will start to occur. The area of the hysteresis loop is calculated from the difference between the areas under the positive and reverse curves. The smaller the size of the hysteresis loop of polarization curve is, the lower the pitting tendency of the material[14]. Otherwise, the more electropositive the potential at which the hysteresis loop is completed is, the less likely it is that pitting corrosion will propagate[15]. In Fig. 1 there was found no hysteresis loop for all cases that meant no pitting corrosion occurred.

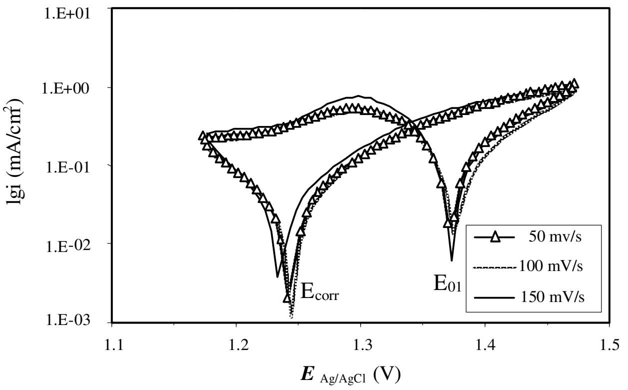

Fig. 1. Cyclic potentiodynamic polarograms of PbO_2-PANi electrodes in 0.5 M H_2SO_4 at scan rate of 5 mV/s (samples prepared by cyclic voltammetry at different scan rates with 300 cycles)

Although the i_{corr} and E_{corr} values given in Table-1 depended weakly on scan rate during material synthesis. In view of corrosion stability they were helping to find out among all regarded samples the best corrosion stability material, which prepared at scan rate of 100 mV/s because of having the positivist E_{corr} as well as E_{o1} resulting the smallest ΔE_o (= E_{o1}- E_{corr}). Additionally, i_{corr} in that case was smaller compared to which at other scan rates. These results were comparable with reported results[10] that this sample having the best uniform morphology among all of the composites.

Cyclic voltammetry: The data on Fig. 2 show that the cyclic voltammetry-diagrams of PANi-PbO_2 composites depended significantly on potential scan rate at which materials were synthesized. For all regarded cases, there were no anodic peak appeared but, two cathodic peaks appeared immediately from the first cycle corresponding to reduction of both α and β-modifications of lead dioxide to lead sulfate at *ca.* 1.1 V and 1.2 V, respectively. In spite of that the reduced peak of α-form in the first cycle was about double higher than that of β-modification, it decreased quickly in the second cycle and disappeared fully after that. Conversely, the β-reduced peak increased strongly following the number of cycle, however, the position of its potential was shifted very lightly on the left side. Additionally, oxidation peaks which illustrated formation of α and β-PbO_2 at about 1.64 V and 1.76 V, respectively, were clearly increasing with cycle number, but, the position of their peak potential seemed to be shifting lightly on the right side.

TABLE-1
KINETIC PARAMETERS FROM CURVES ON FIG. 1 OF PANi-PbO_2 COMPOSITES PREPARED BY CV AT DIFFERENT SCAN RATE FOR 300 CYCLES (MEASURED IN 0.5 M H_2SO_4; POLARIZATION AT 5 mV/s)

Scan rate (mV/s)	i_{corr} (μA/cm²)	E_{corr} (V)	E_{01} (V)	ΔE_o (mV)
50	25.90	1.241	1.371	130
100	25.08	1.255	1.375	120
150	27.63	1.233	1.373	140

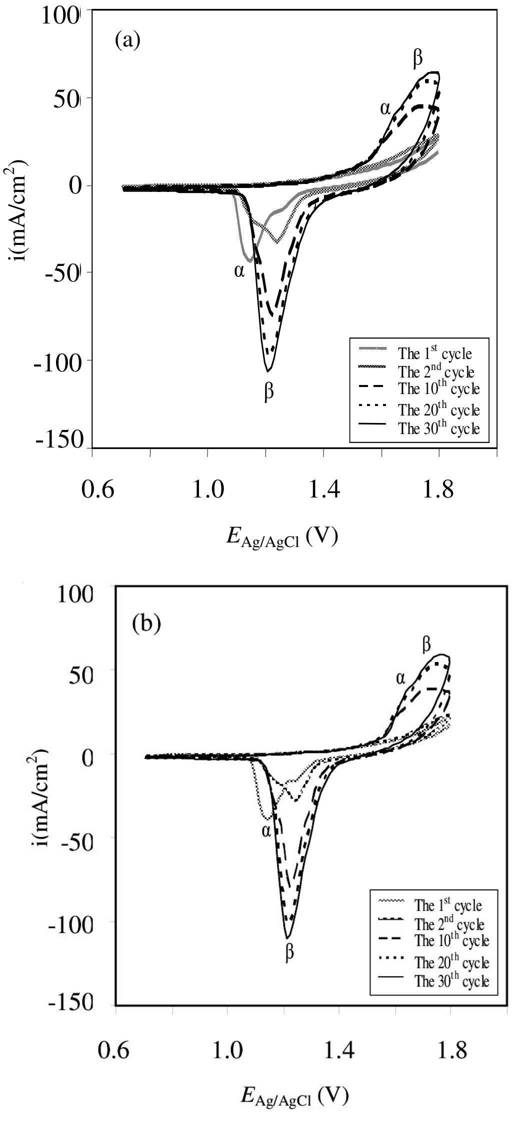

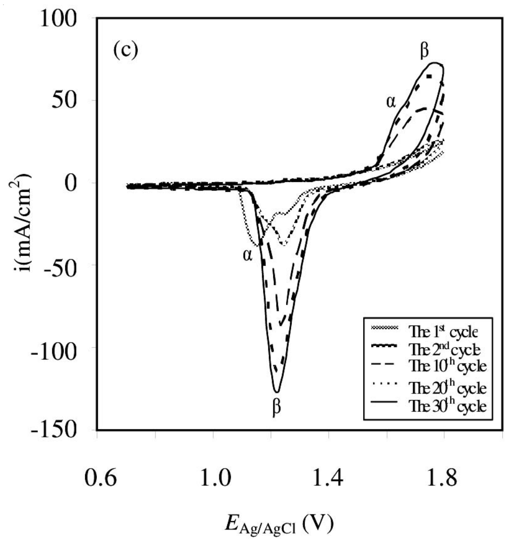

Fig. 2. Cyclic voltammograms of PANi-PbO$_2$ composite in 0.5 M H_2SO_4 at 100 mV/s. Samples prepared from acid medium by cyclic voltammetry at different scan rates: (a) 50 mV/s; (b) 100 mV/s; (c) 150 mV/s

Compared to all of them by voltammograms in the 30th cycle on Fig. 3, it is observed that material prepared at scan rate of 150 mV/s had not only higher redoxidation peak but also positive reduction peak potential than the others. The reason for that can be caused by a presence of PANi in matrix of those composites, which also contributed to co-formation of both α- and β-lead dioxides.

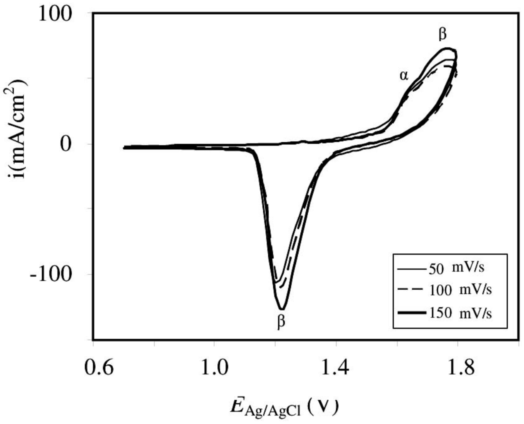

Fig. 3. Cyclic voltammograms in the 30th cycle of PANi-PbO$_2$ composite in 0.5M H_2SO_4 at 100 mV/s. Samples prepared by cyclic voltammetry at differrent scan rates from acid medium

Impedance spectroscopy: Based on results from above cyclic voltammetry-diagrams we chose a potential area of 1.5-1.8 V for impedance study because at which two modifications of α and β-PbO$_2$ formed in anodic direction. Otherwise, we want to explain property of those composites in view of dynamic electrochemistry.

Fig. 4 illustrated that Nyquist plots depended strongly on scan rate at which the material was performanced. Due to simulation from those data there were found two electric equivalent schemas shown in Fig. 5 corresponding to the potential area of 1.5-1.6 V where α-PbO$_2$ formed (a) and another one of 1.7-1.8 V where β-PbO$_2$ could be observed (b). There is dynamically a considerable electrochemical difference between formation of α-PbO$_2$ corresponding schema a on which Warburg diffusion element was found and β-PbO$_2$ corresponding schema b without Warburg diffusion element. It can be explained that an oxidation of Pb^{2+} to Pb^{4+} in α-form occurred only in the potential area of 1.5-1.6 V and then α-PbO$_2$ conversed into β-PbO$_2$ without changing valence. However, this mechanism is suitable for all regarded scan rates during material synthesis.

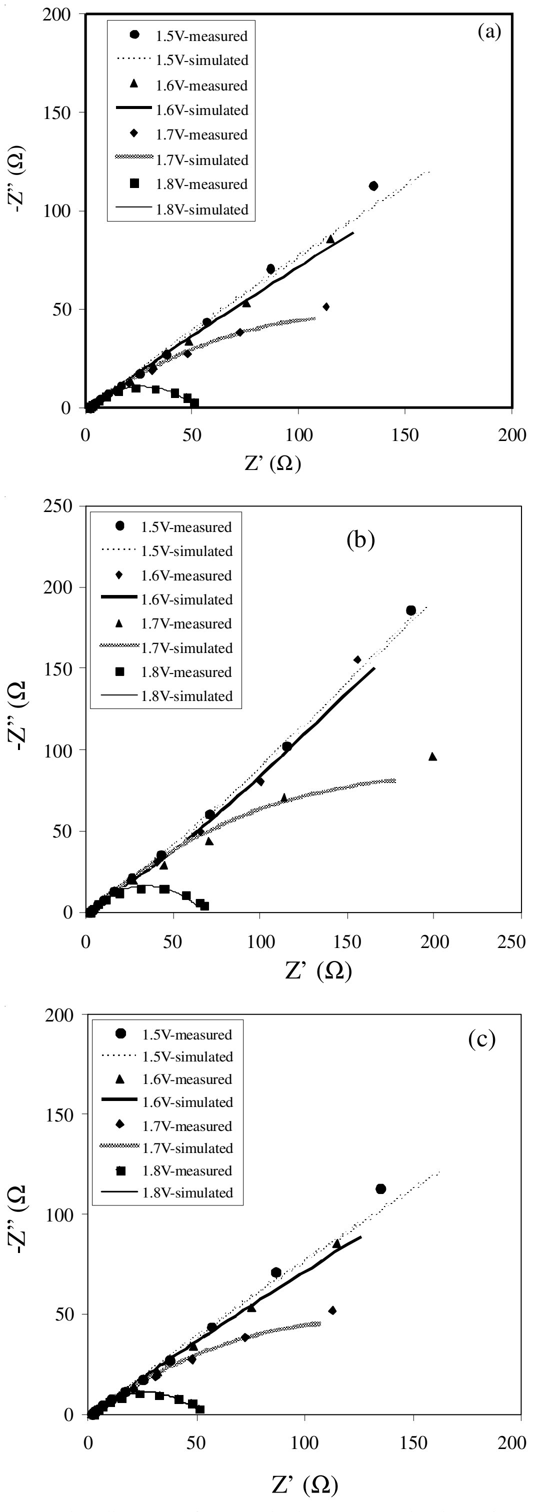

Fig. 4. Nyquist diagrams for PANi-PbO$_2$ composite in 0.5 M H_2SO_4 following potential in oxidation direction from 1.5 V to 1.8 V (frequency range: 100 kHz to 10 mHz; amplitude: 5 mV). Samples prepared by cyclic voltammetry with 300 cycles from acid medium at a scan rate of 50 mV/s (a); 100 mV/s (b); 150 mV/s (c)

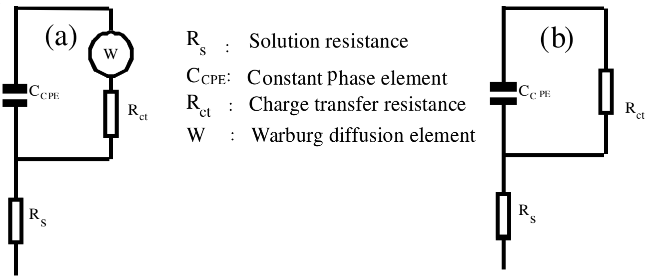

Fig. 5. Electrical simulated circuits belong to Nyquist diagrams from Fig. 4. For potential in oxidation direction from 1.5 V to 1.6 V (a); from 1.7 V to 1.8 V (b)

The data given in Table-2 showed that α-PbO_2 (in potential area from 1.5 V to 1.6 V) was formed more advantageous over β-PbO_2 (in potential area from 1.7 V to 1.8 V) only in the case of material prepared at 100 mV/s because of having smaller R_{ct} than that of β-PbO_2. Otherwise, α-modification in this case appeared very easy due to its smallest charge transfer resistance (66-74 Ω) in comparision with those at other scan rates (1987-2799 Ω for 50 mV/s and 125-140 Ω for 150 mV/s). Additionally, its C_{CPE} values (in potential areas from 1.5 V to 1.7 V) which can be attributed to the charge-transfer reaction were higher than those in both remain cases.

TABLE-2
OBTAINED DATA FROM SIMULATED NYQUIST DIAGRAMS OF PbO_2-PANi ON FIG. 4 FOLLOWING POTENTIAL IN ANODIC DIRECTION

Element	Scan rate (mV/s)	Potential in anodic direction (V)							
		1.5		1.6		1.7		1.8	
R_{ct} (kΩ)	50	2.779		1.987		0.262		0.045	
	100	0.074		0.066		0.398		0.065	
	150	0.125		0.140		0.065		0.144	
σ ($\Omega/s^{1/2}$)	50	16.57		17.51		-		-	
	100	106.70		76.89		-		-	
	150	166.10		129.10		-		-	
		µF	Exp	µF	Exp	µF	Exp	µF	Exp
C_{CPE}	50	188.2	0.44	126.8	0.42	135.7	0.44	166.5	0.53
	100	186.2	0.57	185.6	0.57	150.7	0.50	148.2	0.59
	150	129.7	0.61	131.7	0.58	114.0	0.54	125.6	0.64

The diffusion constant was calculated following equation:

$$D = \frac{2R^2T^2}{n^4F^4A^2C^2\sigma^2} \quad (1)$$

where, σ-Warburg parameter; A-electrode surface area; n-exchange electron number in the charge transfer process; T-absolute temperature, R- Boltzman gas constant; F-Faraday constant; C- Oxidant/reductant concentration of Pb in electrode material [C=1 (mol/cm^3)].

On the basis of above results, Warburg diffusion was found only in the potential area from 1.5 V to 1.6 V where α-PbO_2 was formed. The data shown in Fig. 6 illustrated that the diffusion constant decreased strongly when scan rate increased. However, in the case of potential of 1.6 V compared to that of 1.5 V, it decreased at 50 mV/s and then, raised by increasing scan rate.

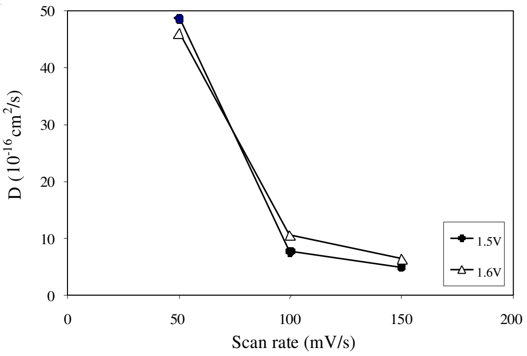

Fig. 6. Dependence of diffusion constant on scan rates during composite synthesis

Conclusion

The above results were generalized to lead to the conclusion that varying scan rate during composite synthesis either redox process or corrosion behaviour of materials was affected. The material prepared at a scan rate of 100 mV/s had the best corrosion stability because of having the smallest corrosion current density and the positive corrosion potential. Due to the presence of PANi in matrix of composites, α-PbO_2 co-existed with β-PbO_2. There was found no diffusion process during formation of β-PbO_2 within cycling.

ACKNOWLEDGEMENTS

This study was financially supported by the NAFOSTED of Vietnam under code number 104.05.58.09. The authors thank the Humboldt-Fellowship for the support of the IM6 equipment.

REFERENCES

1. V.Q. Trung, Ph.D. Dissertation in Chemistry, TU-Dresden, Germany (2006).
2. A.K.C. Gallegos, Ph.D. Thesis, The Material Science Institute of Barcelona, Spain (2003).
3. K.-Q. Ding, *J. Chin. Chem. Soc.*, **56**, 891 (2009).
4. A. Zafar and M. Sadek, Ph.D. Thesis, RMIT University, Melbourne, Australia (2008).
5. L. Zhang and M. Wan, *J. Phys. Chem. B*, **107**, 6748 (2003).
6. P.T. Binh, M.T.T. Thuy and B.H. Ninh, *Vietnam J. Chem.*, **45(6A)**, 31 (2007) (in Vietnamese).
7. S.G. Pawar, S.L. Patil, M.A. Chougule, B.T. Raut, D.M. Jundale and V.B. Patil, *Arch. Appl. Sci. Res.*, **2**, 194 (2010).
8. H. Nur, I.I. Misnon and L.K. Wei, *Internat. J. Photoener.*, Article ID 98548 (2007).
9. P.T. Binh, B.H. Ninh and M.T.T. Thuy, *Vietnam J. Chem.*, **47(6B)**, 137 (2009) (in Vietnamese).
10. P.T. Binh, M.T.T. Thuy, N.X. Truong and T.H. Yen, *Asian J. Chem.*, **23**, 3445 (2011).
11. E.E. Stansbury and R.A. Buchanan, Fundamentals Electrochemical Corrosion, ASM International (2000).
12. M.D. Ralph, T. DeBold and M.J. Johnson, in ed.: J.R. Davis, Corrosion of Stainless Steel, Corrosion. Materials Park, OH, USA:ASM International, pp. 561-564 (1987).
13. M. Darabara, L. Bourithis, S. Zinelis and G.D. Papadimitriou, *Int. Endodontic J.*, **37**, 705 (2004).
14. C. Chandle, M. Kharshan and A. Furman, *Corros. Rev.*, **20**, 379 (2002).
15. ASTM Designation: G61-86, Standard Test Method for Conducting Cyclic Potentiodynamic Polarization Measurements for Localized Corrosion Susceptibility of Iron-, Nickel-, or Cobalt-based Alloys, Annual Book of ASTM Standards, Reapproved, pp. 240-244 (1998).